Engineering Geology 103 (2009) 13–22

Contents lists available at ScienceDirect

Engineering Geology

journal homepage: www.elsevier.com/locate/enggeo

Simplified DMT-based methods for evaluating liquefaction resistance of soils

Pai-Hsiang Tsai [a], Der-Her Lee [a,b], Gordon Tung-Chin Kung [b,*], C. Hsein Juang [c]

[a] Department of Civil Engineering, National Cheng Kung University, Tainan 701, Taiwan
[b] Sustainable Environment Research Center, National Cheng Kung University, Tainan 70944, Taiwan
[c] Department of Civil Engineering, Clemson University, Clemson, SC 29634-0911, USA

ARTICLE INFO

Article history:
Received 17 September 2007
Received in revised form 17 July 2008
Accepted 22 July 2008
Available online 29 July 2008

Keywords:
Liquefaction
Liquefaction potential
Dilatometer test
Standard penetration test
Cone penetration test
Earthquake
Regression analysis

ABSTRACT

This paper presents simplified dilatometer test (DMT)-based methods for evaluation of liquefaction resistance of soils, which is expressed in terms of cyclic resistance ratio (CRR). Two DMT parameters, horizontal stress index (K_D) and dilatometer modulus (E_D), are used as an index for assessing liquefaction resistance of soils. Specifically, CRR–K_D and CRR–E_D boundary curves are established based on the existing boundary curves that have already been developed based on standard penetration test (SPT) and cone penetration test (CPT). One key element in the development of CRR–K_D and CRR–E_D boundary curves is the correlations between K_D (or E_D) and the blow count (N) in the SPT or cone tip resistance (q_c) from the CPT. In this study, these correlations are established through regression analysis of the test results of SPT, CPT, and DMT conducted side-by-side at each of five sites selected. The validity of the developed CRR–K_D and CRR–E_D curves for evaluating liquefaction resistance is examined with published liquefaction case histories. The results of the study show that the developed DMT-based models are quite promising as a tool for evaluating liquefaction resistance of soils.

1. Introduction

Simplified procedures to evaluate the liquefaction potential of soils generally consist of two steps: 1) to evaluate the *loading* to a soil caused by an earthquake and 2) to evaluate the *resistance* of a soil to triggering of liquefaction. The former is generally performed through an estimate of the cyclic stress ratio (CSR) as defined by the pioneering work of Seed and Idriss (1971). The latter is usually accomplished through an estimate of the cyclic resistance ratio (CRR). Because of the difficulty of sampling, CRR is generally determined with simplified methods, such as standard penetration test (SPT)-based methods (e.g., Seed and Idriss, 1971; Seed et al., 1985; Youd et al., 2001; Idriss and Boulanger, 2006), cone penetration test (CPT)-based methods (e.g., Robertson and Campanella, 1985; Robertson and Wride, 1998; Juang et al., 2003; Idriss and Boulanger, 2006), and shear wave velocity (V_s)-based methods (e.g., Andrus and Stokoe, 2000).

Although simplified methods based on SPT, CPT, and V_s are well established, and these *in situ* tests are well developed, use of dilatometer test (DMT) for liquefaction resistance evaluation has received a greater attention in recent years (e.g., Monaco et al., 2005, Monaco and Marchetti, 2007). The DMT is capable of measuring horizontal stresses and has an excellent operational repeatability. Thus, any improvement to the existing DMT-based methods for liquefaction resistance evaluation should be of interest to geotechnical engineers.

The focus of this paper is to develop a new DMT-based model for determining liquefaction resistance of soils. Because of the lack of a large database of case histories at sites where DMT measurements are available, the simplified DMT-based model is developed in this study based on a careful examination of the correlations between the DMT parameters and the parameters of the SPT and the CPT. These correlations along with the existing SPT- and CPT-based liquefaction boundary curves (i.e., CRR models) enable the establishment of the DMT-based boundary curves. The developed DMT-based model is then validated with case histories where the DMT measurements are available. These case histories include those published in the literature as well as those obtained in this study.

2. Existing simplified procedures for evaluating liquefaction potential of soils

A brief overview of the existing simplified procedures is presented in this section. The cyclic stress ratio (CSR) is defined by Seed and Idriss (1971). Depending on how the components of the CSR model are formulated, several forms of CSR formulation have been published. The "consensus" of the CSR formulation is described in Youd et al. (2001), and a more recent update is provided by Idriss and Boulanger (2006). Juang et al. (2006) found that the CSR calculated based on the recommendation of Youd et al. (2001) is very comparable with that recommended by Idriss and Boulanger (2006) for case histories they

* Corresponding author. Tel.: +886 6 384 0136x210; fax: +886 6 384 0960.
E-mail address: tckung@mail.ncku.edu.tw (G.T.-C. Kung).

0013-7952/$ – see front matter © 2008 Elsevier B.V. All rights reserved.
doi:10.1016/j.enggeo.2008.07.008

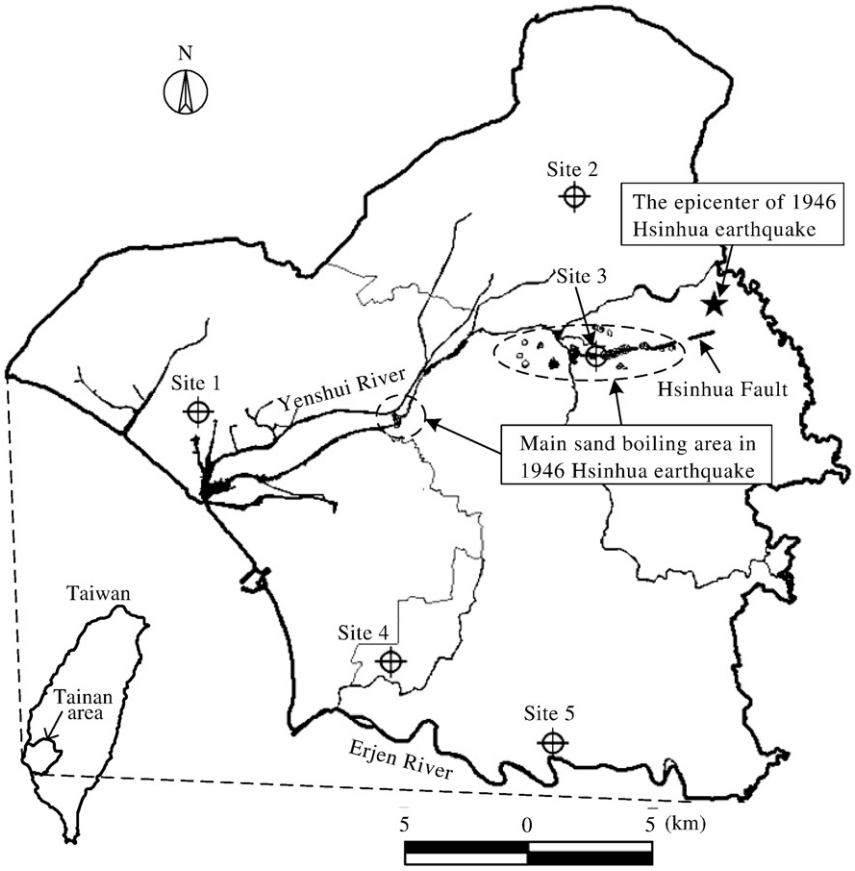

Fig. 1. Layout of five study sites in Tainan.

analyzed. Thus, in this study, the formulation recommended by Youd et al. (2001) is employed.

2.1. Estimate of CRR

The commonly-used SPT- and CPT-based methods as well as the existing DMT-based methods for estimating the CRR are briefly described as follows:

(1) SPT-based methods:

Youd et al. (2001) proposed an update of the CRR curve by Seed et al. (1985), which is expressed as:

$$\mathrm{CRR}_{7.5} = \frac{1}{34-(N_1)_{60cs}} + \frac{(N_1)_{60cs}}{135} + \frac{50}{\left(10(N_1)_{60cs}+45\right)^2} - \frac{1}{200} \tag{1}$$

where $N_{1,60cs}$ is the clean-sand equivalence of the corrected SPT blow count as per Youd et al. (2001). The subscript 7.5 in the $\mathrm{CRR}_{7.5}$ term indicates that this cyclic liquefaction resistance is evaluated at a moment magnitude of 7.5. Note that Eq. (1) is valid only for $N_{1,60cs}<30$, while the sandy soil is considered un-liquefiable when $N_{1,60cs}$ is greater than 30.

Idriss and Boulanger (2006) noted that the trend of the CRR curve proposed by Youd et al. (2001) would sharply increase as the $N_{1,60cs}$ value approaches 30, which may be irrational and would cause the unreasonable results when conducting the probabilistic analysis. They proposed a new model as follows (Idriss and Boulanger, 2006):

$$\mathrm{CRR}_{7.5} = \exp\left\{\frac{(N_1)_{60cs}}{14.1} + \left(\frac{(N_1)_{60cs}}{126}\right)^2 - \left(\frac{(N_1)_{60cs}}{23.6}\right)^3 + \left(\frac{(N_1)_{60cs}}{25.4}\right)^4 - 2.8\right\}. \tag{2}$$

(2) CPT-based methods:

The CPT-based model proposed by Robertson and Wride (1998) is expressed by:

$$\mathrm{CRR}_{7.5} = 0.833\left[\frac{q_{c1N,cs}}{1000}\right] + 0.05 \quad \text{for } q_{c1N,cs}<50 \tag{3a}$$

$$\mathrm{CRR}_{7.5} = 93\left[\frac{q_{c1N,cs}}{1000}\right]^3 + 0.08 \quad \text{for } 50\le q_{c1N,cs}<160 \tag{3b}$$

where $q_{c1N,cs}$ is the clean-sand equivalence of the corrected cone tip resistance as per Robertson and Wride (1998).

(3) DMT-based methods:

The DMT-based methods for evaluating CRR include those by Marchetti (1982), Robertson and Campanella (1986), Reyna and Chameau (1991), Monaco et al. (2005), Grasso and Maugeri (2006), and Monaco and Marchetti (2007). The more recent development by Monaco et al. (2005), Grasso and Maugeri (2006), and Monaco and Marchetti (2007) are briefly reviewed herein.

Monaco et al. (2005) proposed a new CRR curve based on a study of the correlations between cone tip resistance (q_c) and relative density (Dr), between blow count (N) and Dr, and between DMT horizontal stress index (K_D) and Dr. Their DMT-based model is expressed as follows:

$$\mathrm{CRR}_{7.5} = 0.0107K_D^3 - 0.0741K_D^2 + 0.2169K_D - 0.1306. \tag{4}$$

Grasso and Maugeri (2006) further updated the CRR model by Monaco et al. (2005) into:

$$\mathrm{CRR}_{7.5} = 0.0908K_D^3 - 1.0174K_D^2 + 3.8466K_D - 4.5369 \tag{5a}$$

$$\mathrm{CRR}_{7.5} = 0.0308e^{0.6054K_D} \tag{5b}$$

$$\mathrm{CRR}_{7.5} = 0.0111K_D^{2.5307}. \tag{5c}$$

Table 1
Physical properties of soils at Site 1

Depth (m)	USCS	Component of soil (%)			Natural moisture content	Plasticity index	Unit weight	Specific gravity
		Sand	Silt	Clay	w_n (%)	PI (%)	γ_t (kN/m^3)	G_s
1.50	No sample	N/A	N/A	N/A	N/A	N/A	N/A	N/A
3.00	No sample	N/A	N/A	N/A	N/A	N/A	N/A	N/A
4.50	No sample	N/A	N/A	N/A	N/A	N/A	N/A	N/A
6.25	SM	85.6	7.6	6.8	19.6	NP	19.65	2.65
7.50	SM	86.8	7.2	6.0	20.4	NP	19.65	2.65
9.25	SM	87.9	5.5	6.6	19.2	NP	19.65	2.65
10.50	SM	86.6	6.8	6.6	20.1	NP	19.65	2.64
12.00	SM	69.7	22.0	8.3	19.5	NP	19.65	2.66
13.50	SP–SM	92.1	1.4	6.5	23.5	NP	18.86	2.64
15.25	SM	63.2	17.2	19.6	19.2	NP	19.65	2.66
16.50	CL	12.3	38.3	49.4	22.1	22.1	18.86	2.71
18.55	SM	78.9	11.6	9.5	26.3	NP	19.65	2.66
19.50	SM	87.7	5.5	6.8	22.6	NP	19.65	2.65

Table 3
Physical properties of soils at Site 3

Depth (m)	USCS	Component of soil (%)			Natural moisture content	Plasticity index	Unit weight	Specific gravity
		Sand	Silt	Clay	ωn (%)	PI (%)	γ_t (kN/m^3)	G_s
1.20	SM	50.7	39.9	9.4	27.6	NP	17.30	2.68
2.70	ML	36.2	48.0	15.8	21.9	NP	18.86	2.69
4.20	SM	53.6	33.3	13.1	20.9	NP	18.86	2.68
6.05	CL	2.4	59.4	38.2	32.4	15.4	18.86	2.72
7.20	SM	65.4	27.4	7.2	20.6	NP	18.86	2.67
8.70	No sample	N/A	N/A	N/A	N/A	N/A	N/A	N/A
10.45	SM	67.7	24.0	8.3	22.6	NP	18.86	2.66
11.70	SM	54.6	32.8	12.6	21.9	NP	19.65	2.68
13.20	CL	0.7	68.2	31.1	27.8	9.2	18.86	2.72
14.70	ML	43.5	47.1	9.4	22.4	NP	18.86	2.68
16.45	CL	8.0	50.5	41.5	29.0	11.0	18.86	2.72
17.70	CL–ML	6.1	55.7	38.2	25.4	7.0	18.86	2.72
19.20	CL	11.0	51.3	37.7	27.2	11.8	18.86	2.72

Eqs. (5a)–(5c) were generated based on the correlations, Dr–q_c (Bladi et al., 1986), Dr–q_c (Jamiolkowsi et al., 1985), and Dr–N (Gibbs and Holtz, 1957), respectively. Note that all the existing DMT-based methods for evaluating the CRR are based on the correlations between q_c–Dr–K_D and N–Dr–K_D. As such, it is desirable to establish the correlations between q_c–K_D and N–K_D based *directly* on the *in situ* test results, as opposed to indirectly through the use of Dr.

In addition, Monaco and Marchetti (2007) explored the aging effect of *in situ* soils on liquefaction resistance. Comparing with the CPT- and SPT-based evaluation, the DMT evaluation was shown to be able to reflect such effect reasonably. They concluded that the DMT is a suitable tool for the evaluation of liquefaction potential.

3. Development of $N_{1,60cs}$–K_D, $q_{c1N,cs}$–K_D, $N_{1,60cs}$–E_D, and $q_{c1N,cs}$–E_D correlations

3.1. In situ test program

The purpose of *in situ* test program was to obtain data that can be used to establish the correlations among the parameters of three types of *in situ* tests, SPT, CPT, and DMT. In this regard, side-by-side testing with these three types of *in situ* tests was conducted at selected historical earthquake sites. Fig. 1 shows five sites located in Tainan, Taiwan, where evidences of liquefaction (sand boiling) were observed in the 1946 Hsinhwa earthquake. In addition, these sites are in the vicinity of the Tainan High-tech Industrial Park, one of the most critical high-tech manufactory facilities in Taiwan.

The three types of *in situ* tests (SPT, CPT, and DMT) were performed side by side at each of the five sites and the test results were employed to establish the correlations between the key parameters. For DMT, the horizontal stress index (K_D) and dilatometer modulus (E_D), as per Marchetti et al. (2001), were derived; and for SPT and CPT, the commonly-used parameters, $N_{1,60cs}$ and $q_{c1N,cs}$ were derived. Note that at each site, SPT was performed at a depth interval of 1.5 m, while CPT and DMT were conducted at depth intervals of 0.05 m and 0.2 m, respectively. It is noted that when comparing CPT with DMT, the results of CPT sounding were shown only at a depth interval of 0.2 m, not at every 0.05 m as in the sounding profile.

All tests were conducted to the depth of 20 m. The groundwater level at each of the five sites was obtained through the open-end observation well. It is noted that for each test, the standard test methods as described in ASTM (ASTM D 1586-99, 1999; ASTM D 5778-95, 2000; ASTM D 6635-01, 2001) were followed. For SPT, energy ratio at all sites was measured using the standard test method described in ASTM (ASTM D 4633-86, 1986) and all applicable corrections were made according to the recommendation made by Youd et al. (2001). For CPT, the electronic cone and associated devices manufactured by Hogentogler installed in a 20-tons truck are used.

3.2. Results of in situ tests

Tables 1–5 show basic physical properties of soils, including soil classification (USCS), components of soils, natural moisture content (ω_n), plasticity index (PI), unite weight (γ_t), specific gravity of soil (G_s) at each of the five sites. These soil properties were determined from disturbed samples taken from the boreholes. The stratigraphy profile of each of the five sites as well as the key parameters of SPT, CPT, and DMT, including SPT–N value, fines content (FC), soil behavior type

Table 2
Physical properties of soils at Site 2

Depth (m)	USCS	Component of soil (%)			Natural moisture content	Plasticity index	Unit weight	Specific gravity
		Sand	Silt	Clay	ωn (%)	PI (%)	γ_t (kN/m^3)	G_s
2.00	No sample	N/A	N/A	N/A	N/A	N/A	N/A	N/A
3.50	ML	4.5	59.4	36.1	22.4	NP	19.65	2.72
5.00	CL	9.2	52.5	38.3	25.4	11.9	19.65	2.71
6.55	CL	11.5	55.1	33.4	25.1	15.2	18.86	2.71
8.80	ML	8.2	75.5	16.3	23.7	NP	19.65	2.70
11.25	ML	46.7	40.2	13.1	23.4	NP	19.65	2.68
12.50	SM	73.0	20.5	6.5	24.2	NP	19.65	2.65
14.00	SM	55.2	28.9	15.9	19.5	NP	19.65	2.67
15.90	SM	86.3	7.5	6.2	20.4	NP	19.65	2.65
17.00	SM	87.2	6.3	6.5	18.9	NP	19.65	2.65
18.50	CL	0.7	69.7	29.6	29.1	44.4	19.65	2.72
20.00	SC	67.5	22.6	9.9	22.2	7.4	19.65	2.66

Table 4
Physical properties of soils at Site 4

Depth (m)	USCS	Component of soil (%)			Natural moisture content	Plasticity index	Unit weight	Specific gravity
		Sand	Silt	Clay	ωn (%)	PI (%)	γ_t (kN/m^3)	G_s
1.50	No sample	N/A	N/A	N/A	N/A	N/A	N/A	N/A
3.00	ML	27.1	23.7	49.2	15.5	NP	18.86	2.69
4.50	ML	41.7	23.6	34.7	7.2	NP	18.86	2.69
6.00	CL	12.7	49.6	37.7	31.6	7.9	18.86	2.72
7.50	SM	85.7	8.3	6.0	22.3	NP	19.65	2.65
9.15	SM	87.2	5.8	7.0	19.6	NP	19.65	2.65
10.50	SM	78.9	14.1	7.0	20.7	NP	18.86	2.66
12.00	SM	62.3	26.7	11.0	19.2	NP	19.65	2.66
14.45	ML	43.0	47.6	9.4	22.7	NP	19.65	2.69
16.85	SM	50.4	42.6	7.0	23.2	NP	19.65	2.67
18.00	SM	61.2	32.0	6.8	27.0	NP	19.65	2.66

Table 5
Physical properties of soils at Site 5

Depth (m)	USCS	Component of soil (%)			Natural moisture content	Plasticity index	Unit weight	Specific gravity
		Sand	Silt	Clay	ωn (%)	PI (%)	γ_t (kN/m3)	G_s
2.80	CL	19.0	40.0	41.0	15.6	18.7	18.86	2.72
4.30	CL	20.9	41.4	37.7	16.4	12.2	18.86	2.72
5.95	SM	78.4	14.5	7.1	23.2	NP	18.86	2.66
7.30	ML	1.8	39.3	58.9	36.3	NP	17.30	2.73
8.80	CL	33.9	43.8	22.3	22.6	20.9	18.86	2.70
10.55	ML	26.2	41.9	31.9	26.3	NP	18.86	2.70
11.80	SM	81.3	12.7	6.0	23.0	NP	19.65	2.65
13.30	SM	65.1	27.7	7.2	23.7	NP	19.65	2.66
14.95	SM	65.7	27.5	6.8	26.3	NP	19.65	2.66
16.30	SM	55.4	33.6	11.0	19.9	NP	19.65	2.67
17.80	SM	72.1	20.7	7.2	21.1	NP	19.65	2.65
19.45	SM	78.2	14.7	7.1	23.4	NP	19.65	2.65

index (I_c), cone tip resistance (q_c), material index (I_D), dilatometer modulus (E_D), horizontal stress index (K_D), the clean-sand equivalence of standard penetration resistance ($N_{1,60cs}$), and the clean-sand equivalence of normalized cone penetration resistance ($q_{c1N,cs}$), are shown in Figs. 2–6. Those results of SPT, CPT, and DMT measurements, shown in Figs. 2–6, will be available at http://www.serc.org.tw.

Overall, Figs. 2–6 reveal that the pattern of the variation of N values with depth is similar to those of q_c values from CPT and K_D and E_D values from DMT. The results suggest that it may be feasible to establish the correlations between K_D and $N_{1,60cs}$, between E_D and $N_{1,60cs}$, between K_D and $q_{c1N,cs}$, and between E_D and $q_{c1N,cs}$.

3.3. Establishment of $N_{1,60cs}$–K_D, $q_{c1N,cs}$–K_D, $N_{1,60cs}$–E_D, and $q_{c1N,cs}$–E_D correlations

Two scenarios of correlations may be developed herein: 1) K_D and E_D versus the raw parameters, N and q_c, and 2) K_D and E_D versus the corrected parameters, $N_{1,60cs}$ and $q_{c1N,cs}$. In this study, the later is adopted because of the desire to develop a DMT-based model for liquefaction resistance evaluation. Figs. 7 and 8 show the results of both $N_{1,60cs}$–K_D and $q_{c1N,cs}$–K_D correlations as well as $N_{1,60cs}$–E_D and $q_{c1N,cs}$–E_D correlations, respectively, based on the data obtained from the five sites. Note that the terms $N_{1,60cs}$ and $q_{c1N,cs}$ are calculated here based on the formula presented in Youd et al. (2001) and Robertson and Wride (1998), respectively. The best fitted curves of these correlations are obtained as follows:

For the correlations related to K_D:

$$N_{1,60cs} = 0.185K_D^3 - 2.75K_D^2 + 17K_D - 15 \quad (6a)$$

$$q_{c1N,cs} = 0.4K_D^3 - 7.7K_D^2 + 56K_D - 20. \quad (6b)$$

For the correlations related to E_D:

$$N_{1,60cs} = 0.00022E_D^3 - 0.02E_D^2 + 0.9E_D + 3 \quad (7a)$$

$$q_{c1N,cs} = 0.00078E_D^3 - 0.095E_D^2 + 5E_D + 7. \quad (7b)$$

The coefficients of determination (R^2) for Eqs. (6a), (6b), (7a), and (7b) are 0.40, 0.39, 0.53, and 0.54, respectively. Slightly stronger correlation with E_D than with K_D may be attributed to the fact that K_D is noticeably sensitive to factors such as stress history (e.g., OCR), aging, cementation and structure (Jamiolkowsi et al., 1985; Huang and Ma, 1994; Monaco and Marchetti, 2007). It is noted that the regression results shown in Figs. 7 and 8 have a significant scatter. This is not unexpected, as the data are derived from different types of *in situ* testing with different resolutions. These data may also be affected by the actual soil variability, although they are measured side-by-side. However, the trends revealed in these plots are quite strong and clear, and they are considered suitable for developing simplified DMT-based methods. Nevertheless, these empirical, regression-based models should be viewed as the "first-order approximations" and further improvements upon these models are warranted.

The accuracy of K_D as obtained from Eqs. (6a) and (b) can be examined with field measurement at a given site. Fig. 9 shows such a comparison of the computed versus measured K_D at Site No. 1. Also shown in this figure are the results obtained using the empirical model by Grasso and Maugeri (2006). The correlations proposed in this study appear to be able to provide a reasonable estimate of K_D based on either SPT or CPT data. Similar results are obtained at other sites. Thus, the proposed correlations are considered acceptable for

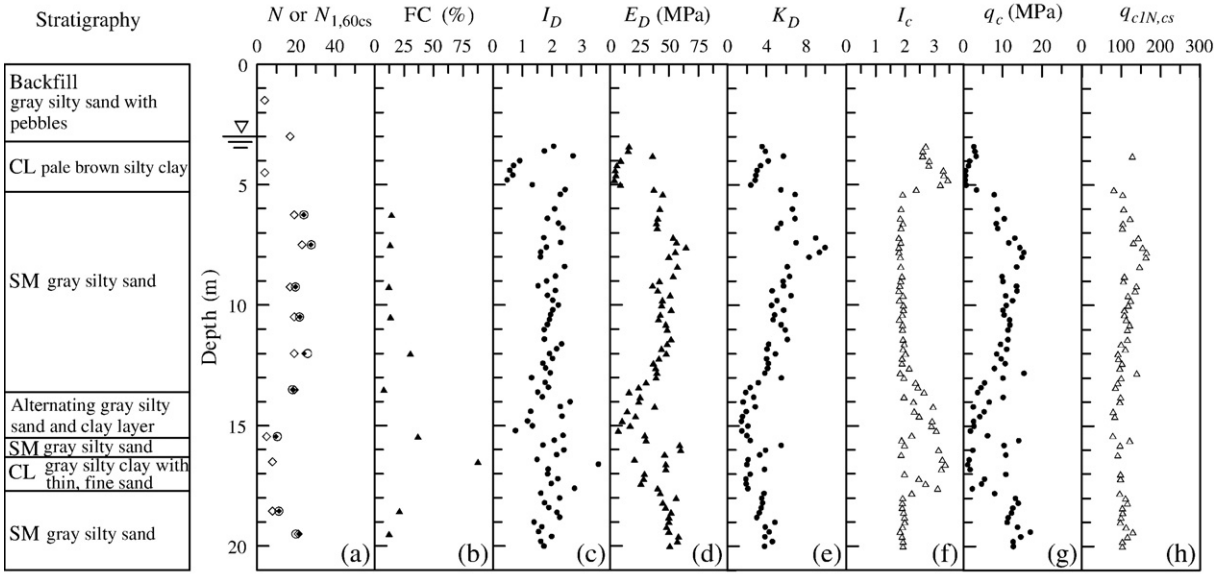

Note: 1. Symbols used in (a) denote (◇ N value ○ $N_{1,60cs}$ using Youd et al. (2001) ◆ $N_{1,60cs}$ using Idriss and Boulanger (2006)
2. Data points in (f) and (h) are estimated using Robertson and Wride (1998)

Fig. 2. Profile of stratigraphy and test results at Site 1.

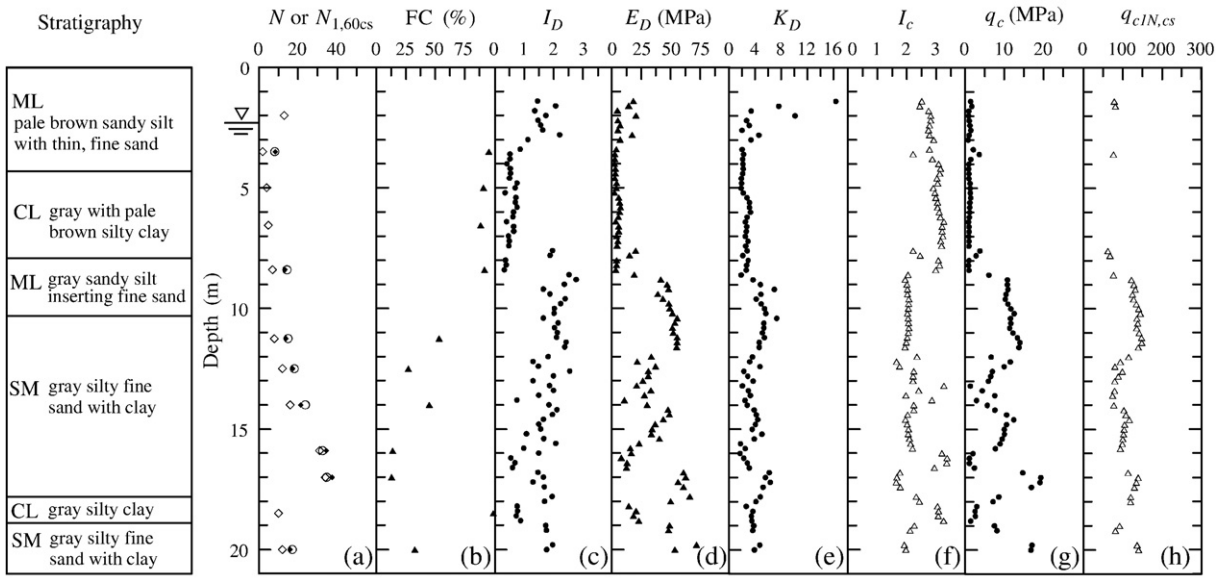

Note: 1. Symbols used in (a) denote (◇ N value ○ $N_{1,60cs}$ using Youd et al. (2001) ◆ $N_{1,60cs}$ using Idriss and Boulanger (2006)
2. Data points in (f) and (h) are estimated using Robertson and Wride (1998)

Fig. 3. Profile of stratigraphy and test results at Site 2.

the purpose of establishing the liquefaction boundary curve through the existing SPT- and CPT-based boundary curves.

4. Establishment of CRR–K_D and CRR–E_D boundary curves

Based on the widely accepted SPT- and CPT-based CRR models Eqs. (1)–(3) and the correlations between various parameters (Eqs. (6a) and (b) and (7a) and (b)), the CRR–K_D and CRR–E_D boundary curves can be derived. Fig. 10 shows the CRR–K_D curves that are "transformed" from Eqs. (1)–(3a) and (b). The difference between the two curves that are based on SPT Eqs. (1) and (2) is quite insignificant, and the difference between those based on SPT and that based on CPT Eqs. (3a) and (b) is relatively insignificant when K_D is less than 5, and becomes more significant with $K_D > 5$.

To further examine these CRR–K_D curves, the data sets of the SPT- and CPT-based liquefaction case histories presented by Idriss and Boulanger (2006) and Robertson and Wride (1998), respectively, are also transformed into Fig. 10. Based on the transformed SPT- and CPT-based CRR–K_D curves along with the transformed data points of the SPT- and CPT-based liquefaction case histories, a new DMT-based CRR–K_D curve is proposed and expressed by:

$$\mathrm{CRR}_{7.5} = \exp\left[\left(\frac{K_D}{8.8}\right)^3 - \left(\frac{K_D}{6.5}\right)^2 + \left(\frac{K_D}{2.5}\right) - 3.1\right]. \quad (8)$$

Finally, the proposed CRR–K_D curve is compared with those published in the literature, as shown in Fig. 11. Note that the data shown in this figure are again the "transformed" data points of the

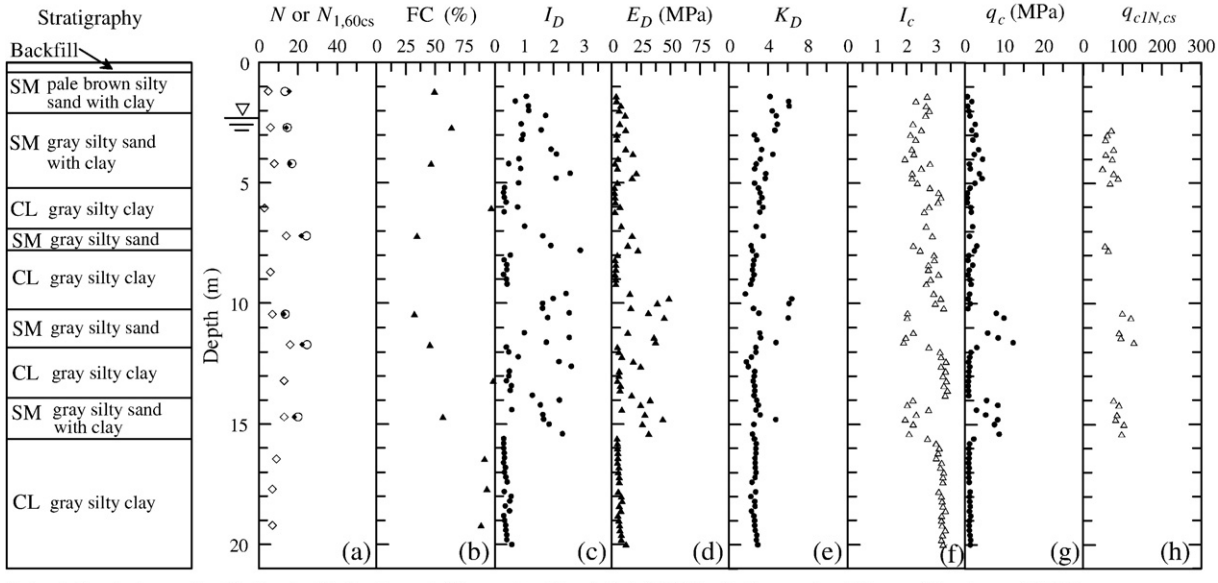

Note: 1. Symbols used in (a) denote (◇ N value ○ $N_{1,60cs}$ using Youd et al. (2001) ◆ $N_{1,60cs}$ using Idriss and Boulanger (2006)
2. Data points in (f) and (h) are estimated using Robertson and Wride (1998)

Fig. 4. Profile of stratigraphy and test results at Site 3.

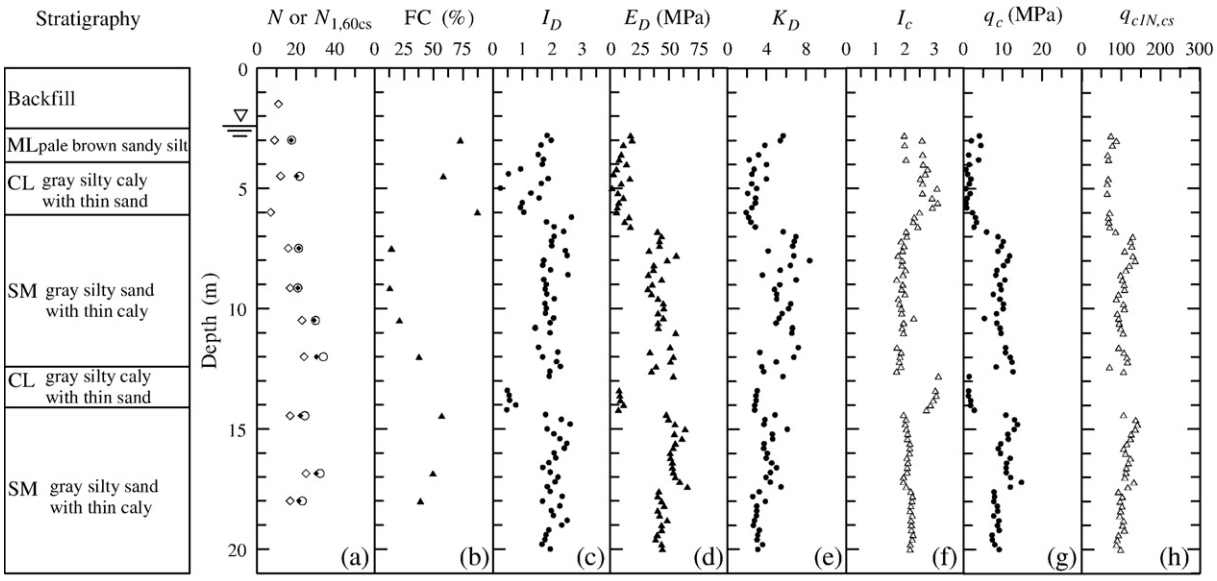

Note: 1. Symbols used in (a) denote (◇ N value ○ $N_{1,60cs}$ using Youd et al. (2001) ◆ $N_{1,60cs}$ using Idriss and Boulanger (2006)
2. Data points in (f) and (h) are estimated using Robertson and Wride (1998)

Fig. 5. Profile of stratigraphy and test results at Site 4.

existing liquefaction case histories presented by Idriss and Boulanger (2006) and Robertson and Wride (1998). The proposed CRR–K_D curve appears to be superior to the previously published CRR–K_D curves.

Similar to the CRR–K_D curve, the CRR–E_D curve can be transformed from the existing boundary curves Eqs. (1)–(3a) and (b)). Fig. 12 shows the CRR–E_D curves that are "transformed" from Eqs. (1)–(3a) and (b). The difference between the two curves that are based on SPT Eqs. (1) and (2) is quite insignificant, and the difference between those based on SPT and that based on CPT Eqs. (3a) and (b) is relatively insignificant when E_D is less than 50, and becomes more significant with $E_D > 50$.

Again, based on the transformed SPT- and CPT-based CRR–E_D curves along with the transformed data points of the SPT- and CPT-based liquefaction case histories, a new DMT-based CRR–E_D curve is proposed and expressed by

$$\mathrm{CRR}_{7.5} = \exp\left[\left(\frac{E_D}{49}\right)^3 - \left(\frac{E_D}{36.5}\right)^2 + \left(\frac{E_D}{23}\right) - 2.7\right]. \quad (9)$$

It is noted that the difference in the CRR–E_D curves between those transformed from the SPT-based boundary curves and those from the CPT-based curves is significantly less than the difference in the CRR–K_D curves with the corresponding transformations. Further examination of this finding is warranted; however, the results suggest that the CRR–E_D curve may be more capable of reflecting liquefaction resistance behavior than the CRR–K_D curve.

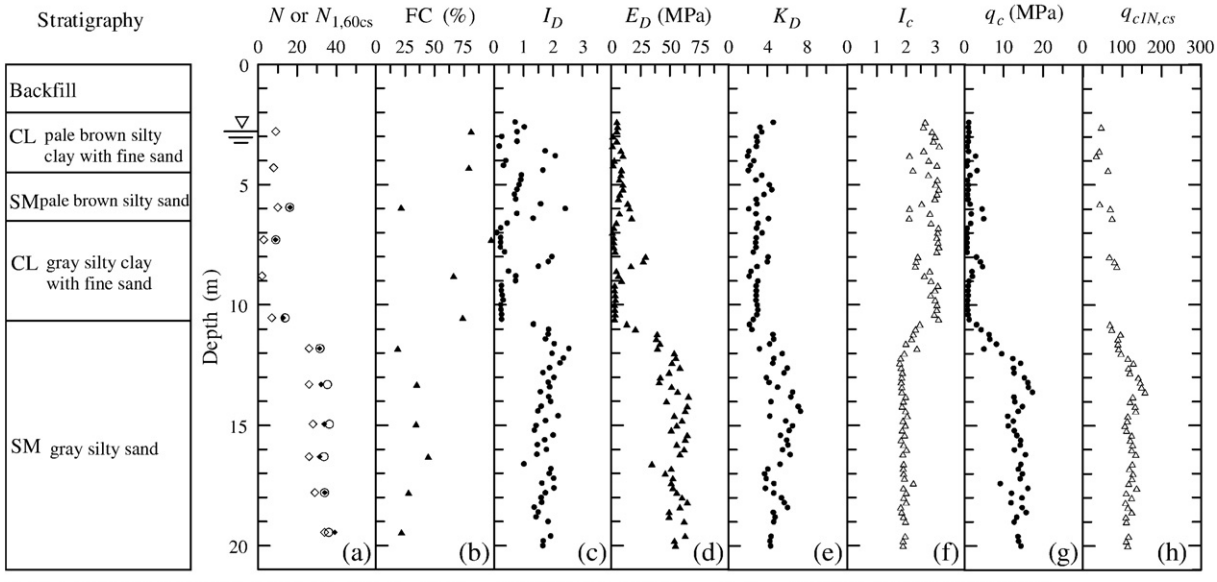

Note: 1. Symbols used in (a) denote (◇ N value ○ $N_{1,60cs}$ by Youd et al. (2001) ◆ $N_{1,60cs}$ by Idriss and Boulanger (2006)
2. Data points in (f) and (h) are estimated by Robertson and Wride (1998)

Fig. 6. Profile of stratigraphy and test results at Site 5.

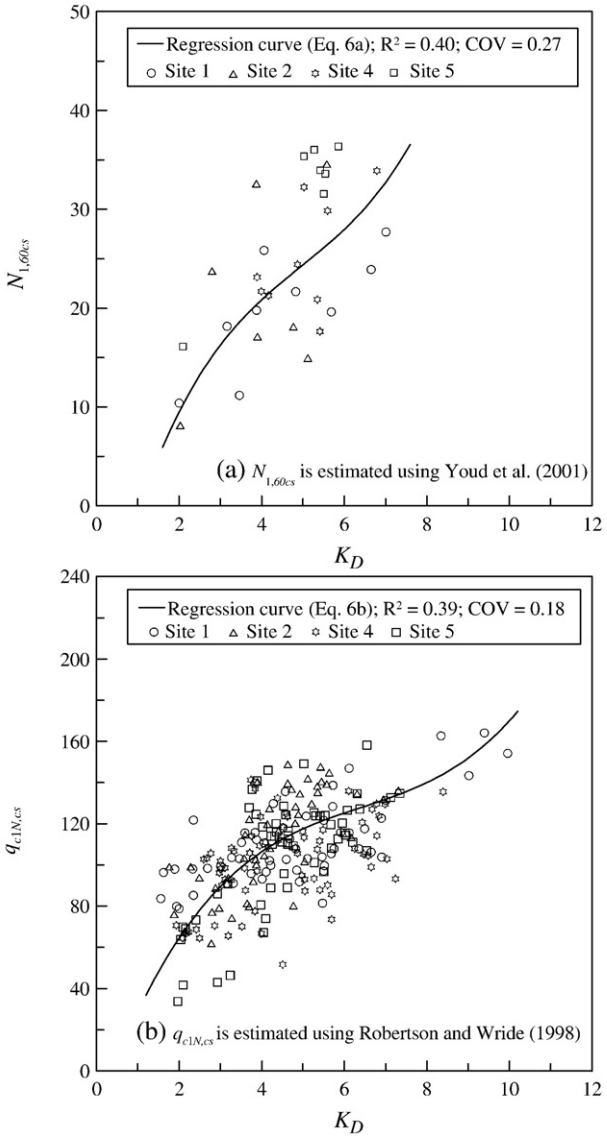

Fig. 7. Relationships between $q_{c1N,cs}$–K_D and $N_{1,60cs}$–K_D.

Before validating the developed CRR–K_D and CRR–E_D curves, it is desirable to investigate the effect of variability of the developed models (Eqs. (6a) and (b) and (7a) and (b)) on the accuracy of liquefaction evaluation. To this end, a sensitivity analysis is conducted with some variations in these empirical models to investigate its effect on the liquefaction boundary curves Eqs. (8) and (9). Although not shown herein, the results indicate that the change in the obtained boundary curves is practically negligible.

5. Validation of developed DMT-based CRR models

To validate the developed DMT-based CRR models Eqs. (8) and (9), the DMT data performed in a liquefied site presented by the past studies (e.g., Renya and Chameau, 1991; Mitchell et al., 1994) and in a liquefied site conducted in this study (Site 3; see Fig. 1) are analyzed. In addition, the four sites (Sites 1, 2, 4, and 5; see Fig. 1), where no liquefaction characteristics were reported during 1946 Hsinhwa earthquake, are also examined. For the historic site in the former case, the reader is referred to Reyna and Chameau (1991) and Mitchell et al. (1994) for details, whereas the sites in the latter case are summarized in the following.

Site 3 in this study is located in the main soil boiling area during the 1946 Hsinhwa earthquake (see Fig. 1). According to Cheng et al. (1999), the moment magnitude of this earthquake is M_w=6.1; the epicenter is at N23.07 and E120.33; and the observed earthquake intensity is V. The maximum peak ground acceleration (PGA) in the main soil boiling area is estimated to be 250 gal (Cheng et al., 1999). The location (Site 3), where the *in situ* tests were performed, was selected based on results of the past study (Chang et al., 1947) and the records of liquefaction phenomena preserved at the administration building of the town of Hsinhwa. Field investigation conducted in this study revealed that the pattern of farmland activities in the main soil boiling area has not been changed in the past several decades.

Fig. 13 shows the particle size distribution of sandy soils at various depths at Site 3. The upper and lower bounds for most liquefiable and potentially liquefiable soils proposed by Ishihara et al. (1980) and the upper and lower bounds for liquefied soils established for the 1999 Chi-Chi earthquake by NCREE (2000) are also shown in Fig. 13. The particle size distributions of silty sand (SM) layers at Site 3 mostly fall in the range suggested by Ishihara et al. (1980) for liquefiable soils, and completely fall into the range established for the 1999 Chi-Chi earthquake.

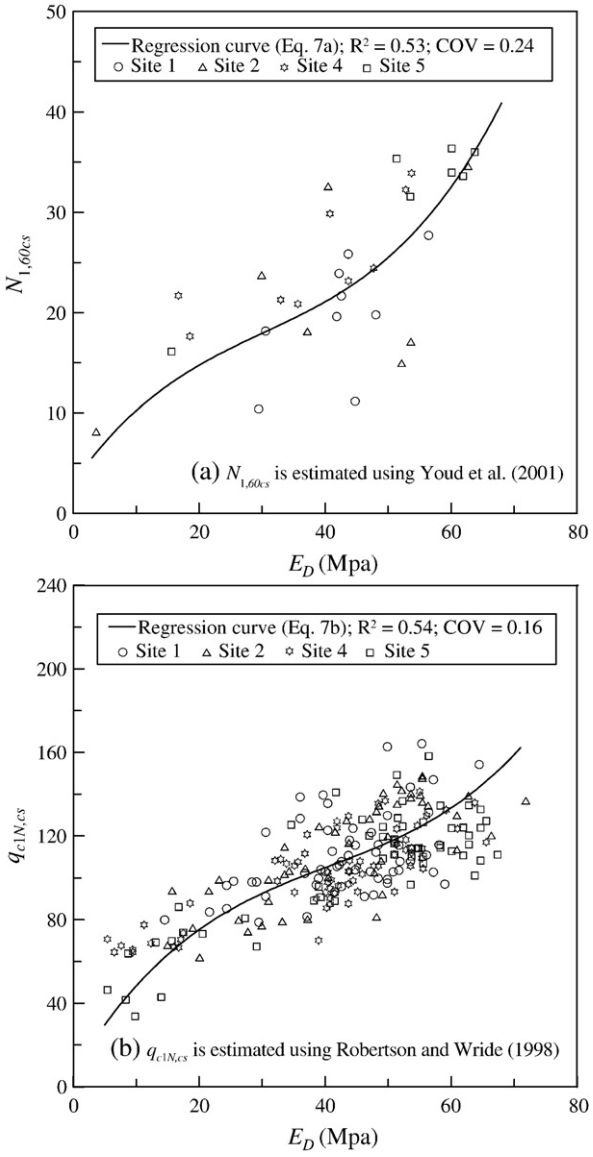

Fig. 8. Relationships between $q_{c1N,cs}$–E_D and $N_{1,60cs}$–E_D.

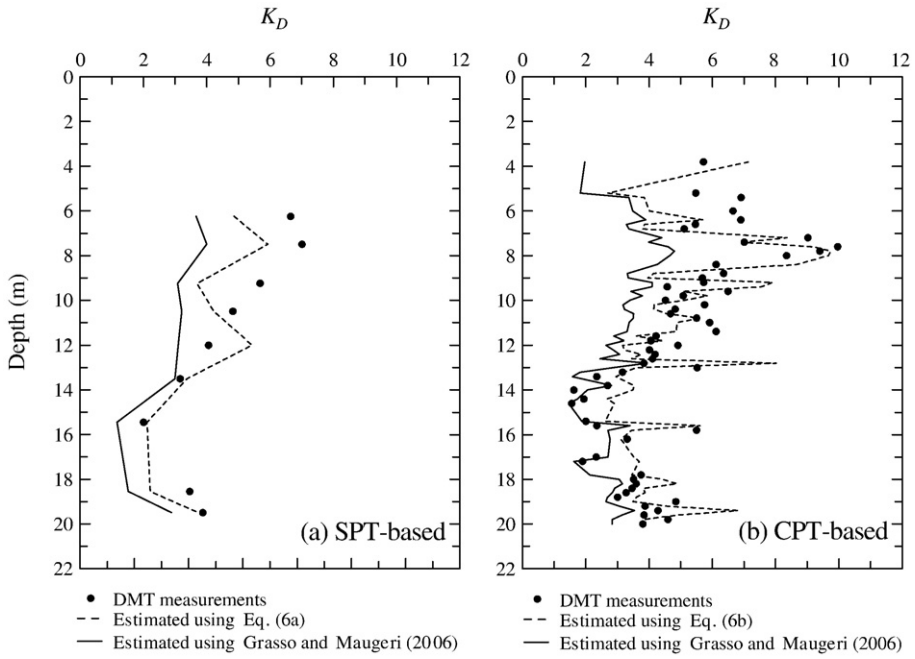

Fig. 9. Comparison of performance of q_c–K_D and N–K_D correlations proposed in this study and using Grasso and Maugeri (2006) on estimate of K_D observed at Site 1.

The factor of safety against the occurrence of liquefaction, generally defined as FS=CRR/CSR, at each of the five SM layers is obtained based on the SPT and CPT data, as shown in Fig. 14. In these analyses, the groundwater level is assumed to be at the depth of 0.5 m. Note that the five SM layers at this site are denoted as SM1, SM2… and SM5, respectively. Based on the SPT-data, the factor of safety in SM1 and SM2 is equal to or slightly less that 1.0, where as it is greater than 1.0 in the other three SM layers. Based on CPT data, however, the factor of safety is all less than 1.0. Field observations reported by Chang et al. (1947) indicated that silt was observed in the boiling soils in the main soil boiling area (Fig. 1) and the colors of the boiled soils were primarily pale brown and gray. Thus, the SM2 layer is judged to be the critical layer, where the liquefaction most probably had been triggered at this site.

Liquefaction phenomena were not reported at Sites 1, 2, 4, and 5 in the 1946 Hsinhwa earthquake. The observed earthquake intensity is V at Site 2 and IV at Sites 1, 4, and 5. The PGA is estimated to be 250 gal at Site 2 and 80 gal at Sites 1, 4, and 5 (Cheng et al., 1999). Similar to Site 3, the critical SM layers at each of the other four sites were determined (5.3 m to 13.6 m for Site 1; 9 m to 13.7 m for Site 2; 6.1 m to 12.4 m for Site 4; 4.5 m to 6.5 m for Site 5) and the corresponding DMT results are used to validate the developed CRR curves herein.

Figs. 15 and 16 assess the performance of the developed DMT-based CRR–K_D and CRR–E_D boundary curves with available case histories at sites where DMT measurements are available. Based on limited data, the performance of the developed DMT-based CRR–K_D and CRR–E_D curves appear to be quite satisfactory, although the CRR–E_D curve is not as convincing as the CRR–K_D curve because of the lack

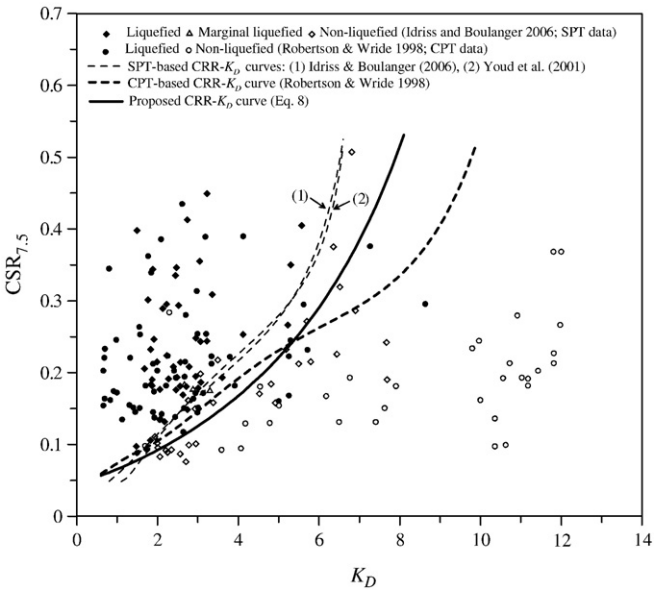

Fig. 10. Establishment of the proposed CRR–K_D curve for clean sand and M=7 1/2.

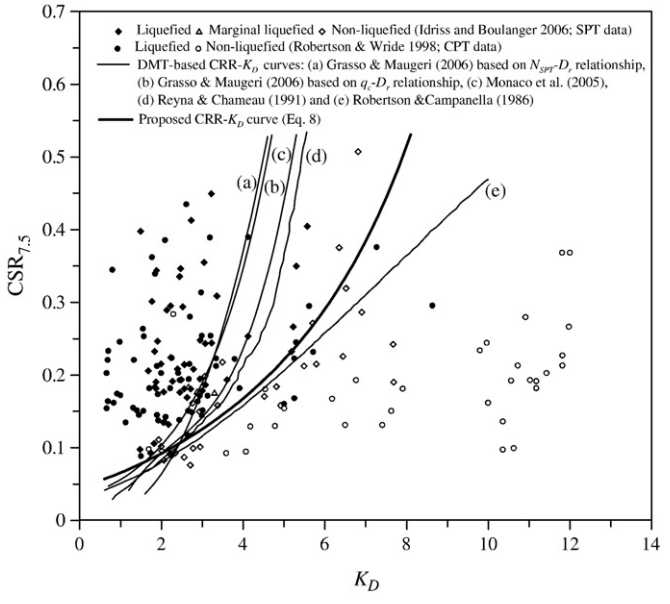

Fig. 11. Comparison of CRR–K_D curves for clean sand and M=7 1/2 between previous studies and this study.

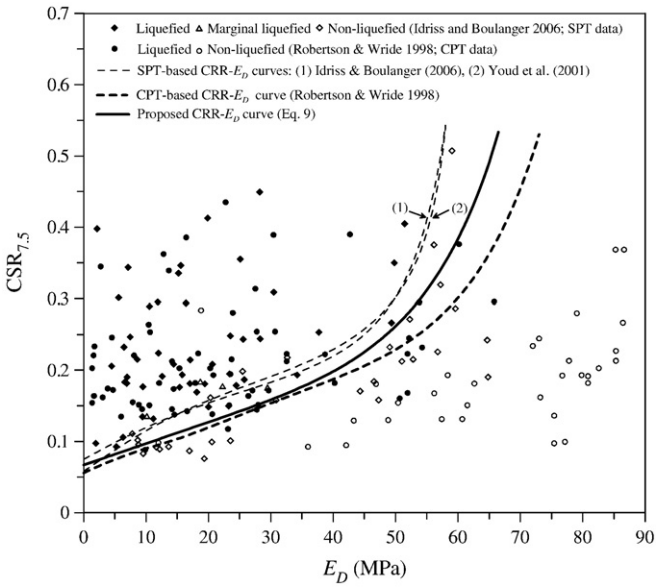

Fig. 12. Establishment of the proposed CRR–E_D curve for clean sand and M=7 1/2.

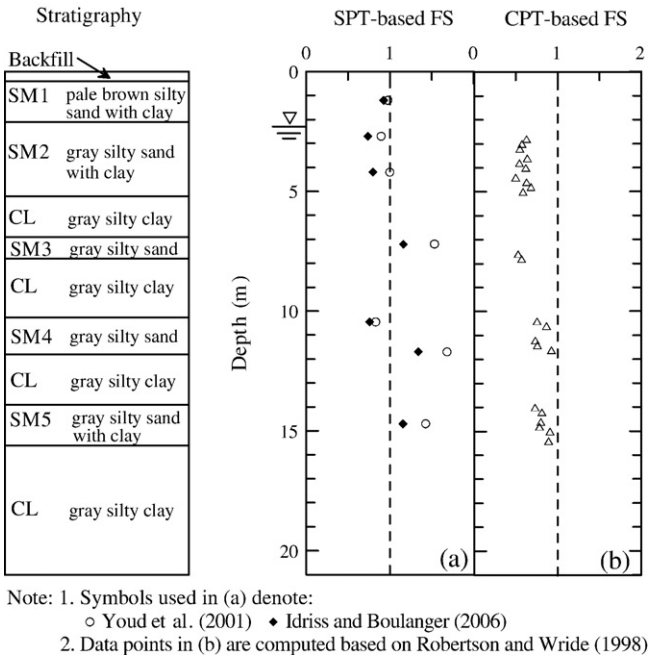

Fig. 14. Profile of the factor of safety for liquefaction according to the SPT and CPT data at Site 3.

of data near the boundary curve. The results show that the DMT-based method for evaluating liquefaction potential of soils is quite feasible and promising. Further collection of quality case histories to validate the developed DMT-based boundary curves is warranted.

6. Conclusions

Simplified SPT- and CPT-based methods for liquefaction potential evaluation are extensively employed. Youd et al. (2001) suggested use of two or more test procedures for liquefaction potential evaluation if possible. In this study, two new DMT-based boundary curves (CRR–K_D and CRR–E_D) were developed. Based on the results of this study, the following conclusions may be drawn:

1. The CRR–K_D and CRR–E_D boundary curves were developed for evaluating liquefaction resistance of soils based on the existing SPT- and CPT-based boundary curves and the correlations between $q_{c1N,cs}$–K_D, $N_{1,60cs}$–K_D, $q_{c1N,cs}$–E_D, and $N_{1,60cs}$–E_D, respectively. The developed CRR–K_D and CRR–E_D curves have been preliminarily validated with case histories collected in the past studies and the present study. Further collection of quality case histories to validate the developed DMT-based boundary curves is warranted.
2. In the previous studies, only the horizontal stress index (K_D) has been used to develop the DMT-based boundary curve. However, the results of this study suggest that E_D may be more suitable than K_D to be correlated with CRR, as reflected by the observation that the correlation of $q_{c1N,cs}$–E_D and $N_{1,60cs}$–E_D are "stronger" than that of $q_{c1N,cs}$–K_D and $N_{1,60cs}$–K_D. This result may be attributed to the fact that K_D is noticeably sensitive to factors such as stress history (e.g., OCR), aging, pure prestraining, cementation and structure (Monaco et al., 2005), whereas E_D, $N_{1,60cs}$, and $q_{c1N,cs}$ are less sensitive to those factors (Marchetti, 1982; Huang and Ma, 1994; Jamiolkowsi et al., 1985). However, further studies to investigate this finding are warranted.

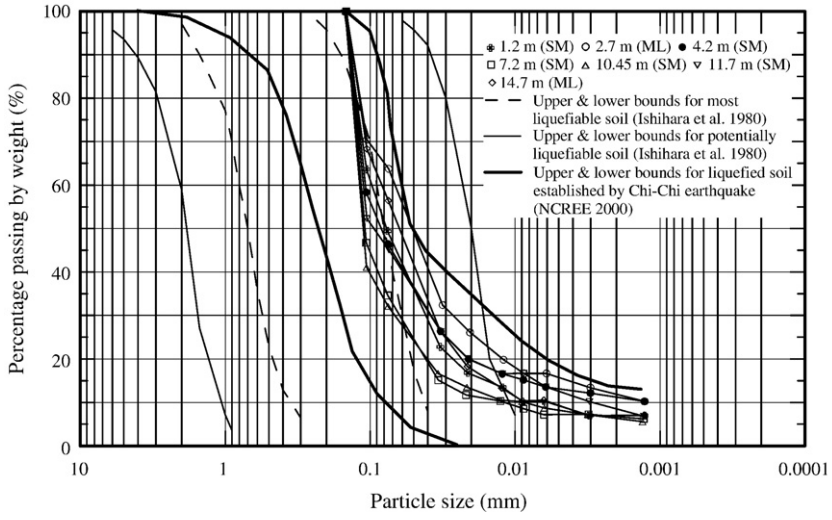

Fig. 13. Particle size distribution curves of soils at Site 3.

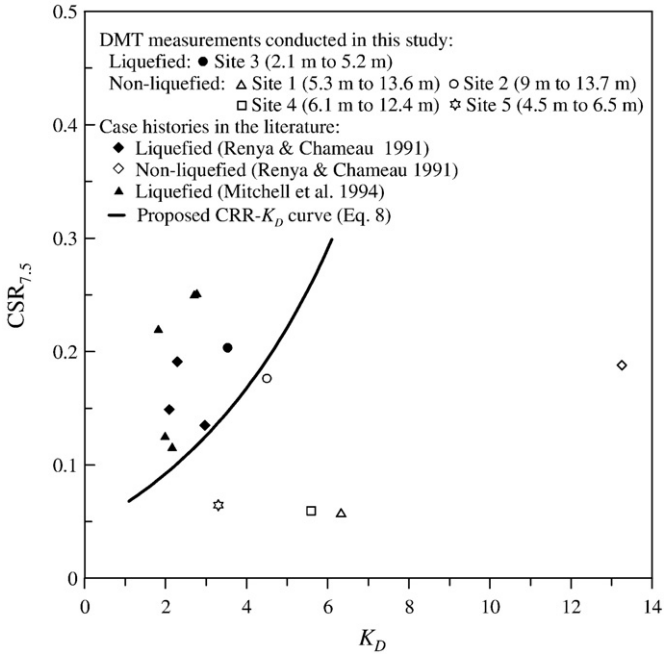

Fig. 15. Validation of the proposed DMT-based CRR–K_D curve using the case histories presented in the literature and conducted in this study.

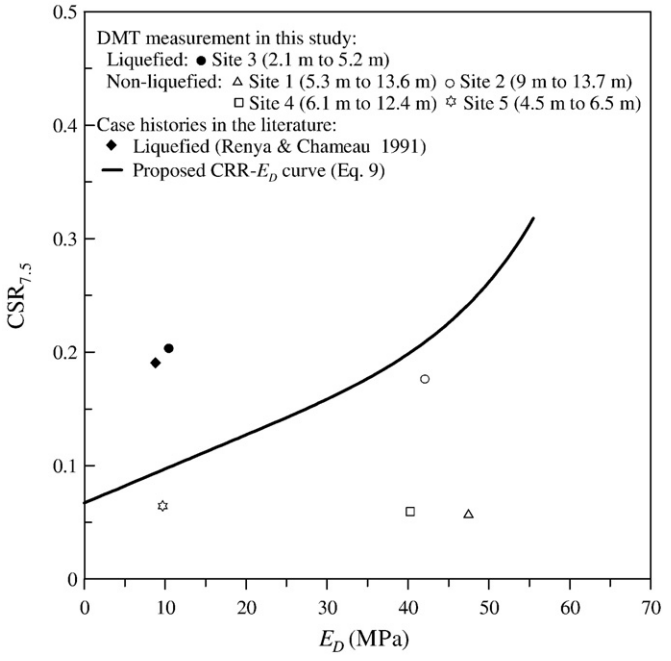

Fig. 16. Validation of the proposed DMT-based CRR–E_D curve using the case histories presented in the literature and conducted in this study.

3. The $q_{c1N,cs}$–K_D and $N_{1,60cs}$–K_D correlations established in this study were built on the previous studies (e.g., Grasso and Maugeri, 2006). Based on the field tests conducted in this study, the new $q_{c1N,cs}$–K_D and $N_{1,60cs}$–K_D correlations appear to show some improvements over the existing such correlations. The corresponding boundary curves developed in this study also show significant improvements.

Acknowledgements

The study on which this paper is based was supported by the Central Geological survey, MOEA of Taiwan through Grant No. 592690100-03-9301. This financial support is greatly appreciated. The results and opinions expressed in this paper are those of the writers and do not necessarily represent the view of the Central Geological survey, MOEA of Taiwan. The writers are solely responsible for the results and opinions represented in this paper.

References

Andrus, R.D., Stokoe, K.H., 2000. Liquefaction resistance of soils from shear-wave velocity. Journal of Geotechnical and Geoenvironmental Engineering 126 (11), 1015–1025.

ASTM D 4633-86, 1986. Standard test method for stress wave energy measurement for dynamic penetrometers. ASTM standard: D 4633-86, Vol. 04.08.

ASTM D 1586-99, 1999. Standard test method for penetration test and split-barrel sampling of soils. Book of Standards, Vol. 04.08.

ASTM D 5778-95, 2000. Standard test method for performing electronic friction cone and piezocone penetration testing of soils. Book of Standards, Vol. 04.08.

ASTM D 6635-01, 2001. Standard test method for performing the flat plate dilatometer. Book of Standards, Vol. 04.09.

Bladi, G., Bellotti, R., Ghionna, V., Jamiolkowsi, M., Pasqualini, E., 1986. Interpretation of CPT and CPTUs. 2nd part: drained penetration of sands. Proc. 4th International Geotechnical Seminar, Singapore, pp. 143–156.

Chang, L.S., Zhou, M., Chen, P.Y., 1947. Tainan earthquake on December 5 of 1946. Bulletin of the Central Geological Survey 1, 11–18.

Cheng, S.N., Yeh, Y.T., Hsu, M.T., Shin, T.C., 1999. Photo album of ten disastrous earthquakes in Taiwan. Central Weather Bureau of Taiwan, Report No. CWB-9-1999-002-9.

Gibbs, K.J., Holtz, W.G., 1957. Research on determining the density of sands by spoon penetration testing. Proc. 4th ICSMFE 1, London, pp. 35–39.

Grasso, S., Maugeri, M., 2006. Using K_D and V_s from seismic dilatometer (SDMT) for evaluating soil liquefaction. Proc. 2nd International Flat Dilatometer Conference, pp. 281–288.

Huang, A.B., Ma, M.Y., 1994. An analytical study of cone penetration tests in granular material. Canadian Geotechnical Journal 31, 91–103.

Idriss, I.M., Boulanger, R.W., 2006. Semi-empirical procedures for evaluating liquefaction potential during earthquakes. Soil Dynamics and Earthquake engineering 26, 115–130.

Ishihara, K., Troncoso, J., Kawase, Y., Takahashi, Y., 1980. Cyclic strength characteristics of tailings materials. Soils and Foundations 20 (4), 127–142.

Jamiolkowsi, M., Baldi, G., Bellotti, R., Ghionna, V., Pasqualini, E., 1985. Penetration resistance and liquefaction of sands. Proc. 11th ICSMFE 4, San Francisco, pp. 1891–1896.

Juang, C.H., Yuan, H., Lee, D.H., Lin, P.S., 2003. Simplified cone penetration test-based method for evaluating liquefaction resistance of soils. Journal of Geotechnical and Geoenvironmental Engineering, ASCE 129 (1), 66–79.

Juang, C.H., Fang, S.Y., Khor, E.H., 2006. First order reliability method for probabilistic liquefaction triggering analysis using CPT. Journal of Geotechnical and Geoenvironmental Engineering, ASCE 132 (3), 337–350.

Marchetti, S., 1982. Detection of liquefiable sand layers by means of quasi-static penetration tests. Proc. 2nd European Symposium on Penetration Testing, Amsterdam, pp. 689–695.

Marchetti, S., Monaco, P., Totani, G., Calibrese, M., 2001. The flat dilatometer (DMT) in soil investigations (ISSMGE TC16). Proc. International Conference on *In-Situ* Measurement of Soil Properties and Case Histories, Bali, Indonesia, pp. 95–131.

Mitchell, J.K., Lodge, A.I., Coutinho, R.Q., Kayen, R.E., Seed, R.B., Nishio, S., Stokoe, K.H., 1994. Insitu test results from four Loma Prieta earthquake liquefaction site: SPT, CPT, DMT and shear wave velocity. Report No. UCB/EERC-94/04, Earthquake Engineering Research Center, University of California, Berkeley.

Monaco, P., Marchetti, S., 2007. Evaluating liquefaction potential by seismic dilatometer (SDMT) accounting for aging/stress history. Proc. 4th International Conference on Earthquake Geotechnical Engineering, Thessaloniki, paper No. 1626, Springer.

Monaco, P., Marchetti, S., Totani, G., Calabrese, M., 2005. Sand liquefiability assessment by Flat Dilatometer Test. Proc. 16th ICSMGE 4, Osaka, pp. 2693–2697.

National Center for Research on Earthquake Engineering, 2000. In: Lin, M.L. (Ed.), Reconnaissance Report on the Seismic Disaster of the 921 Chi-Chi Earthquake About the Geotechnical Engineering, Report No. NCREE-99-053.

Reyna, F., Chameau, J.L., 1991. Dilatometer based liquefaction potential of sites in the Imperial Valley. Proc. 2nd International Conference on Recent Advance in Geotechnical Earthquake Engineering and Soil Dynamics 3.13, St. Louis, Missouri, pp. 385–392.

Robertson, P.K., Campanella, R.G., 1985. Liquefaction potential of sands using the CPT. Journal of Geotechnical Engineering, ASCE 111 (3), 384–403.

Robertson, P.K., Campanella, R.G., 1986. Estimating liquefaction potential of sands using the flat plate dilatometer. Geotechnical Testing Journal 9 (1), 38–40.

Robertson, P.K., Wride, C.E., 1998. Evaluating cyclic liquefaction potential using the cone penetration test. Canadian Geotechnical Journal 35, 442–459.

Seed, H.B., Idriss, I.M., 1971. Simplified procedure for evaluating soil liquefaction potential. Journal of the Soil Mechanics and Foundations Division, ASCE 97, 1249–1273.

Seed, H.B., Tokimatsu, K., Harder, L.F., Chung, R.M., 1985. The influence of SPT procedures in soil liquefaction resistance evaluations. Journal of Geotechnical Engineering, ASCE 111 (12), 1425–1445.

Youd, T.L., Idriss, I.M., Andrus, R.D., Arango, I., Castro, G., Christian, J.T., Dobry, R., Finn, W.D.L., Harder, L.F., Hynes, M.E., Ishihara, K., Koester, J.P., Liao, S.C., Marcuson III, W.F., Martin, G.R., Mitchell, J.K., Moriwaki, Y., Power, M.S., Robertson, P.K., Seed, R.B., Stokoe II, K.H., 2001. Liquefaction resistance of soils: summary report from 1996 NCEER and 1998 NCEER/NSF workshops on evaluation of liquefaction resistance of soils. Journal of Geotechnical and Geoenvironmental Engineering, ASCE 127 (10), 817–833.